PROCEEDINGS OF SCIENCE

Global characteristics of GRBs observed with *INTEGRAL* and the inferred large population of low-luminosity GRBs

Lorraine Hanlon*
School of Physics, University College Dublin, Dublin 4, Ireland.
E-mail: lorraine.hanlon@ucd.ie

Suzanne Foley
School of Physics, University College Dublin, Dublin 4, Ireland.
E-mail: sfoley@bermuda.ucd.ie

Brian McBreen
School of Physics, University College Dublin, Dublin 4, Ireland.
E-mail: brian.mcbreen@ucd.ie

Sinead McGlynn
Department of Physics, KTH, AlbaNova Universitetcentrum, SE 10691 Stockholm, Sweden.
E-mail: smcglynn@particle.kth.se

Sheila McBreen
School of Physics, University College Dublin, Dublin 4, Ireland.
E-mail: sheila.mcbreen@ucd.ie

Antonio Martin-Carrillo
School of Physics, University College Dublin, Dublin 4, Ireland.
E-mail: antonio.martin-carrillo@ucd.ie

PoS(Integral08)011

PROCEEDINGS OF SCIENCE

The γ-ray instruments on board *INTEGRAL* have detected and localised 55 GRBs from launch in October 2002 up to July 2008, including 53 long-duration GRBs ($T_{90} \gtrsim 2$ s) and 2 short-duration GRBs ($T_{90} \lesssim 2$ s).

The spectra of the majority of *INTEGRAL* GRBs can be well described by single power-laws. In 11 cases, models with curvature, such as the Band model or the power law plus blackbody model, are required to fit the time-averaged burst spectra.

INTEGRAL detects proportionally more weak GRBs than Swift because of its higher sensitivity in a smaller field of view. The all-sky rate of GRBs above $\sim$0.15 ph cm^{-2} s^{-1} is $\sim$1400 yr^{-1} in the fully coded field of view of IBIS. Spectral lags i.e. the time delay in the arrival of low-energy γ-rays with respect to high-energy γ-rays, can be measured for 31 of the GRBs in the sample. Two groups are identified in the spectral lag distribution of *INTEGRAL* GRBs, one with short lags $<$0.75 s (between 25–50 keV and 50–300 keV) and one with long lags $>$ 0.75 s. Most of the long-lag GRBs are inferred to have low redshifts because of their tendency to have low peak energies and their faint optical and X-ray afterglows. They are mainly observed in the direction of the supergalactic plane with a quadrupole moment of $Q = -0.225 \pm 0.090$ and hence reflect the local large-scale structure of the Universe. The rate of long-lag GRBs with inferred low luminosity is $\sim$25% of Type Ib/c SNe. Some of these bursts could be produced by the collapse of a massive star without a SN. Alternatively, they could result from a different progenitor, such as the merger of two white dwarfs or a white dwarf with a neutron star or black hole, possibly in the cluster environment without a host galaxy.

7th INTEGRAL Workshop
September 8-11 2008
Copenhagen, Denmark

*Speaker.

PoS(Integral08)011

1. Introduction

The main γ-ray instruments on board *INTEGRAL*, namely IBIS [1] and SPI [2] are optimised for high-resolution imaging and spectroscopy of the γ-ray sky, respectively. The IBIS instrument is comprised of two separate layers of dectectors, ISGRI in the 15 keV–1 MeV energy range [3], and PICsIT in the 180 keV–10 MeV energy range [4]. IBIS/ISGRI has 16384 CdTe detectors, located 3.4 m from a tungsten mask which projects a shadowgram onto the detector plane. Maps of the sky are reconstructed by decoding the shadowgram with the mask pattern. IBIS has a fully coded field of view (FCFoV) of $9^\circ \times 9^\circ$ and a partially coded field of view (PCFoV) of $19^\circ \times 19^\circ$ at 50% coding and $29^\circ \times 29^\circ$ at zero coding. SPI consists of 19 hexagonal germanium (Ge) detectors covering the energy range 20 keV–8 MeV with high energy resolution of 2.5 keV at 1.3 MeV. A coded mask is located 1.71 m above the detector plane for imaging purposes, giving a 16° corner-to-corner FCFoV and a PCFoV of 34°. The SPI and IBIS instruments are supported by an optical camera (OMC, [5]) and an X-ray monitor (JEM-X, [6]).

The *INTEGRAL* Burst Alert System (IBAS[1], [7]) is an automatic ground-based system for the accurate localisation of GRBs and the rapid distribution of GRB coordinates, providing, on average, 0.8 GRBs per month with an error radius of $\sim$3 arcminutes. *INTEGRAL* detected 53 long-duration GRBs ($T_{90} \gtrsim 2$ s) and 2 short-duration GRBs ($T_{90} \lesssim 2$ s) between October 2002 and July 2008. Of the two short bursts, GRB 070707 is a member of the short-hard class [8], while GRB 071017 is a short-duration burst whose location is consistent with the X-ray source AX J1818.8-1559 [9]. *INTEGRAL* bursts of particular interest include the low-luminosity GRB 031203 [10], the very intense GRB 041219a [11] and a number of X-ray rich GRBs such as GRB 040223 [12, 13], GRB 040403 [14] and GRB 040624 [13]. In addition, a bright, hard GRB outside the field of view has been detected using the ISGRI Compton mode [15].

2. Global properties of *INTEGRAL* GRBs

The exposure map and spatial distribution of the 47 GRBs observed with IBIS during the period from October 2002 to July 2007 are shown in galactic coordinates in Fig. 1. The burst distribution is significantly concentrated towards the galactic plane, reflecting the direction in which the satellite is pointed. During this period *INTEGRAL* spent 64% of its observing time in the half of the sky at galactic latitudes between $\pm 30^\circ$.

The T_{90} distribution of *INTEGRAL* GRBs, measured in the 20–200 keV energy range, is shown in Fig. 2 and compared with the bimodal distribution obtained for BATSE GRBs [16]. There is reasonable agreement between the two distributions, especially when the small number of *INTEGRAL* GRBs is taken into account. The IBIS lightcurves of 48 *INTEGRAL* bursts are given in Foley et al. (2008) [17].

2.1 Afterglows of *INTEGRAL* GRBs

The X-ray, optical and radio afterglow detections are listed in Table 1 for a total of 535 GRBs well localised by various missions between July 1996 and July 2008, showing in particular the observed number of afterglows based on *INTEGRAL* GRB detections.

[1] http://ibas.iasf-milano.inaf.it/IBAS_Results.html

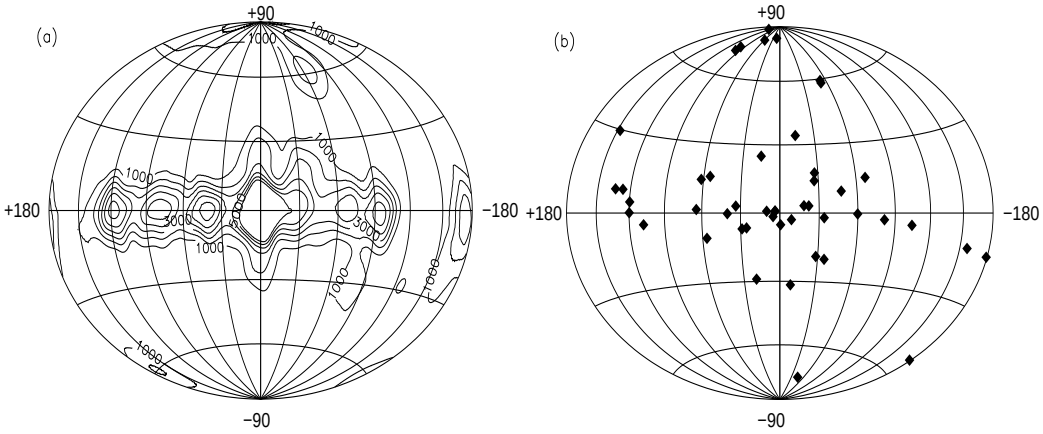

Figure 1: (a) *INTEGRAL* exposure map in galactic coordinates from October 2002 up to July 2007 (contours in units of kiloseconds), showing the concentration of exposure in the direction of the galactic plane (Erik Kuulkers, private communication). (b) Spatial distribution of 47 *INTEGRAL* GRBs detected between October 2002 and July 2007 in galactic coordinates.

Table 1: Total number of GRBs localised by *BeppoSAX*, *HETE-2*, *INTEGRAL* and *Swift* and subsequent afterglow detections at X-ray, optical and radio wavelengths, between July 1996 and July 2008. The data are taken from the webpage maintained by Jochen Greiner at http://www.mpe.mpg.de/∼jcg/grbgen.html.

	BeppoSAX	**HETE-2**	***INTEGRAL***	***Swift***
GRBs	55	79	**55**	342
X-ray	31	19	**21**	294
Optical	17	30	**20**	176
Radio	11	8	**8**	22

Almost 70% of the GRBs observed by *INTEGRAL* do not have a detected optical counterpart. Optical observations revealed faint afterglows for GRB 040323 and GRB 040827, and near-IR afterglows for GRB 040223 and GRB 040624 [13]. The IBIS error box of GRB 060114 contains galaxies from the cluster A1651 ($z = 0.087$) and the optical afterglow was fainter than $R = 19$ just 1.9 min after the GRB [18]. Radio afterglows have been detected for 8 *INTEGRAL* GRBs.

GRB 040223 and GRB 040624 [13] provide good examples of GRBs with dark or faint optical afterglows. GRB 040223 was observed close to the galactic plane, so NIR observations were carried out to overcome the high dust obscuration. Observations were undertaken at the NTT of ESO, 17 hours after the GRB and no afterglow was found. GRB 040624 was located far from the galactic plane at high latitude where the optical extinction is negligible. Afterglow observations were carried out 13 hours after the burst using the VLT and TNG. Magnitude limits were obtained in the optical that are fainter than the very faint end of the distribution of the magnitudes of a compilation of 39 promptly observed counterparts. The position of GRB 040624 is less than $5'$ from a galaxy in the cluster A1651. A search for a supernova was carried out up to a month after the GRB but none was found to a faint limit of $R > 22.6$ [19].

Spectroscopic redshifts have been determined for four *INTEGRAL* GRBs, i.e. GRB 031203 at z=0.1055 [20]; GRB 050223 at z=0.584 [21]; GRB 050525a at z=0.606 [22] and GRB 050502a

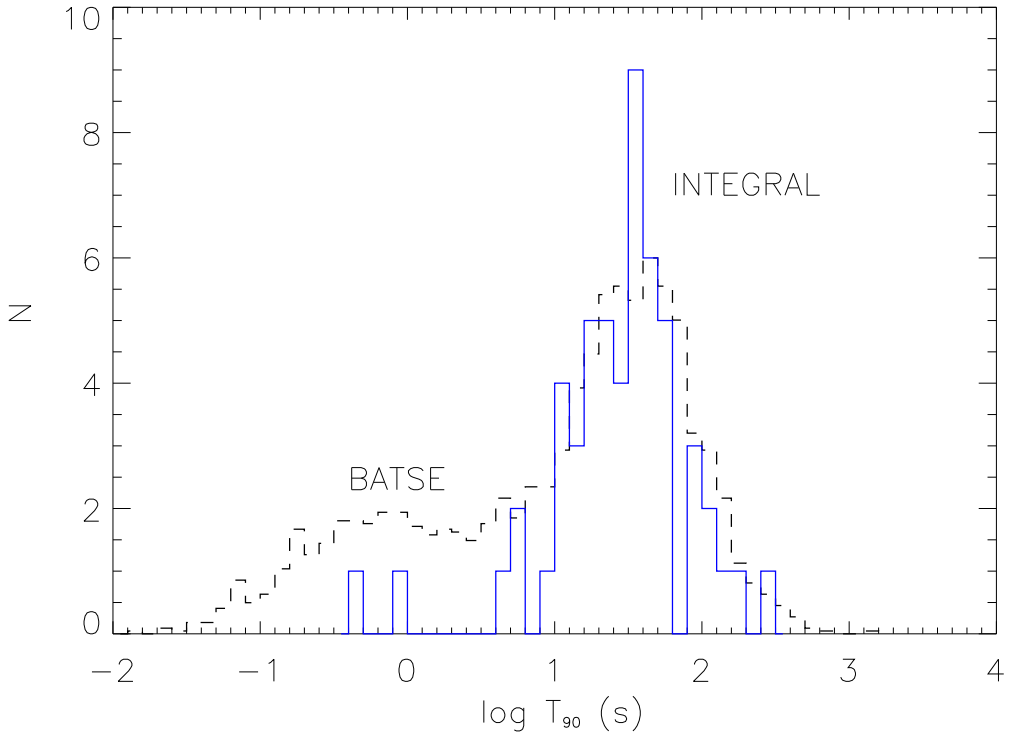

Figure 2: T_{90} distribution of *INTEGRAL* GRBs shown in blue in comparison to that of BATSE (dashed line). The BATSE distribution is normalised to the *INTEGRAL* distribution for clarity. The BATSE data for 2041 GRBs is taken from the Current Catalog at http://www.batse.msfc.nasa.gov/batse/grb/catalog/current.

at z=3.793 [23]. Non-spectroscopic redshifts have been inferred for GRB 040812 ($0.3 < z < 0.7$, [24]) and GRB 040827 ($0.5 < z < 1.7$, [25]). The low efficiency for measuring redshifts is mainly due to the fact that *INTEGRAL* spends a large amount of observing time pointing towards the galactic plane.

There are a number of redshift indicators that can be used for GRBs without direct redshift determinations. One such indicator is the spectral lag which combines the spectral and temporal properties of the prompt GRB emission. The spectral lag is a measure of the time delay between GRB emission in a high-energy γ-ray band relative to the arrival of photons in a low-energy band e.g. [26]. The typical lag values measured for long-duration GRBs detected by the Burst and Transient Source Experiment (BATSE) between the 25–50 keV and 100–300 keV channels concentrate at ~ 100 ms [27]. An anti-correlation between spectral lag and isotropic peak luminosity was first observed by [27], using 6 BATSE bursts with measured redshifts. However, there exist notable outliers, in particular the ultra-low luminosity bursts GRB 980425, GRB 031203 and GRB 060218, associated with the supernovae SN 1998bw, SN 2003lw and SN 2006aj, respectively. Short bursts ($T_{90} < 2$ s) have very small or negligible lags [28] and relatively low peak luminosities and so do not lie on the correlation [29].

3. Spectral Lag Analysis

In order to measure the lag, background-subtracted lightcurves were extracted in three energy bands, 25–50 keV (Channel 1), 50–100 keV (Channel 2) and 100–300 keV (Channel 3). The lag, τ, between two energy channels was determined by computing the cross-correlation function (CCF) between the two lightcurves as a function of temporal lag as described by [30] and [27]. Assuming the time profiles in both energy channels display sufficient similarity, the peak in the CCF then corresponds to the time lag of the GRB between the two energy channels in question. To account for those cases in which the signal level in Channel 3 was insufficient to determine an accurate lag, the counts in Channels 2 and 3 were combined and correlated with Channel 1 to give $\tau_{2+3,1}$. In this paper, GRBs with $\tau_{2+3,1} > 0.75$ s are defined as long-lag.

The CCF was fit with a fourth order polynomial in order to account for the asymmetry of the CCF [27]. The peak of the polynomial fit to the CCF was then taken to be the true lag value. For each GRB, an average spectral lag over the total burst duration was determined. Statistical errors were calculated using a bootstrap method as described in [27]. This involves adding Poissonian noise based on the observed counts to the lightcurves in the different energy channels and re-computing the CCF in 100 realisations for each burst. The 50th ranked value is then the mean lag and the 16th and 84th ranked values represent $\pm 1\sigma$. The lightcurve data was over-resolved by a factor of 10 in order to compute the errors at a time resolution less than the natural binning of the raw data.

4. Results

There are 11 GRBs within the FCFoV of 0.025 sr of IBIS in 4 years of observation time, yielding an all-sky rate of $\sim 1400\,\mathrm{yr}^{-1}$ above the threshold of $\sim 0.15\,\mathrm{ph\,cm^{-2}\,s^{-1}}$ in the energy range 20–200 keV. The rate of GRBs is in good agreement with the values obtained from the more sensitive analysis of BATSE archival data [31, 32]. Fig. 3 (a) compares the peak flux (20–200 keV) distribution of the GRBs observed by IBIS (solid line) to the peak flux (15–150 keV) distribution of the GRBs detected by the BAT instrument on *Swift*. IBIS detects proportionally more weak GRBs than *Swift* because of its better sensitivity within a FoV that is smaller by a factor of ~ 12.

The number distribution of spectral lags measured over the full burst duration is given in Fig. 3 (b) for the 28 long-duration GRBs with a measured lag between Channel 1 (25–50 keV) and Channels 2 & 3 (50–300 keV). No statistically significant negative spectral lags are found. Negative lags, which violate the typical hard-soft evolution of GRBs, have been observed in a small minority of cases [33] and may be more prevalent in short bursts [34]. A long tail extending to ~ 5 s is observed in the lag distribution in Fig. 3 (b) and a clear separation between short and long lag is drawn at $\tau_{2+3,1} \sim 0.75$ s. Thus, long-lag bursts have $\tau_{2+3,1} > 0.75$ s and those with $\tau_{2+3,1} < 0.75$ s are referred to as short-lag GRBs. The spectral lag distribution of *INTEGRAL* GRBs as a function of peak flux is shown in Fig. 4. The BeppoSAX SN burst GRB 980425 [35] is also shown, as is GRB 060505 which has no associated SN [36, 37]. The figure shows that both bright and faint GRBs have short spectral lags, but there is an obvious absence of bright long-lag GRBs. Therefore GRBs with long spectral lags tend to be weak bursts with low peak flux. This trend is in good agreement with that observed using BATSE GRBs [38], where the proportion of long-lag GRBs

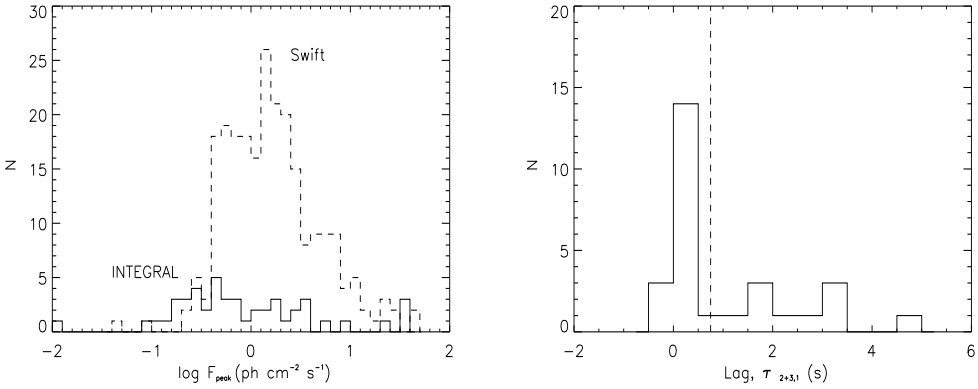

Figure 3: (a) Peak flux distribution for GRBs detected by *INTEGRAL* (20–200 keV, solid line) and *Swift* (15–150 keV, dashed line). The *Swift* data for 237 GRBs is taken from http://swift.gsfc.nasa.gov/docs/swift/archive/grb_table.html. (b) Spectral lag distribution for the 28 *INTEGRAL* GRBs for which a lag could be measured between 25–50 keV and 50–300 keV ($\tau_{2+3,1}$). The distribution is separated by the dashed line into short-lag and long-lag GRBs at $\tau_{2+3,1} = 0.75$ s.

is negligible among bright BATSE bursts and increases to around 50% at the trigger threshold. In order to establish the robustness of the spectral lag analysis, GRB lightcurves with different peak count rates were simulated and offset by a range of lag values. In all cases the spectral lag was successfully recovered for both bright and faint GRBs using the analysis procedure described in § 3.

The isotropic peak luminosity as a function of spectral lag is shown in Fig. 5 and includes the 3 *INTEGRAL* GRBs with known redshift for which a lag was measured. The low-luminosity bursts GRB 980425, XRF 060218 and GRB 060505 are also plotted in Fig. 5. The dashed line is the anti-correlation between lag and luminosity proposed by [27]. The bright *INTEGRAL* bursts GRB 050502a and GRB 050525a follow the trend of the relation. At $z = 0.106$, GRB 031203 has a peak luminosity of 8.4×10^{48} erg s^{-1} and spectral lag of $0.17^{+0.03}_{-0.04}$ s, causing it to fall significantly below the correlation [10, 29].

5. The Population of Long-lag GRBs with Low Luminosities

The median properties of long and short lag *INTEGRAL* GRBs are given in Table 2 for the 28 long-duration bursts with a measured value of $\tau_{2+3,1}$. Approximately 40% of *INTEGRAL* GRBs with a measured lag belong to the long-lag category. The median peak flux for long-lag GRBs is a factor of ~ 5 lower than for GRBs with short lags.

The distribution of the *INTEGRAL* GRBs in supergalactic coordinates is shown in Fig. 6. All of the *INTEGRAL* GRBs are divided almost equally between the half of the sky above and below $\pm 30^\circ$, in agreement with the exposure map which has $\sim 52\%$ of the exposure time within $\pm 30^\circ$ of the supergalactic plane. However, 10 of the 11 long-lag GRBs are concentrated at supergalactic latitudes between $\pm 30^\circ$. The quadrupole moment [39] has a value of $Q = 0.007 \pm 0.043$ for all *INTEGRAL* GRBs and $Q = -0.225 \pm 0.090$ for the long-lag GRBs. The quadrupole moment of the 47 bursts is consistent with zero and an isotropic distribution. The non-zero moment of the long-lag

bursts indicates an anisotropy in the distribution of these GRBs with respect to the supergalactic plane. The binomial probability that this is a chance occurrence is 7×10^{-3}. GRB 980425 and XRF 060218 have long lags and lie within $\pm 30^{\circ}$ of the supergalactic plane, while GRB 031203 has a relatively short lag and lies at a high supergalactic latitude. The long-lag GRBs observed with BATSE are also significantly concentrated in the direction $\pm 30^{\circ}$ of the supergalactic plane with a quadrupole moment $Q = -0.097 \pm 0.038$ [38]. The combined results of more than 14 years of observations with IBIS and BATSE lead us to conclude that long-lag GRBs trace the features of the nearby large-scale structure of the Universe as revealed with superclusters, galaxy surveys [40, 41] and the very high energy cosmic rays [42]. This result is a further indication that most long-lag GRBs are nearby and have low luminosity. The local supercluster seems to be appended to a web of filaments and sheets, rather than an isolated pancake structure, with superclusters evident to $\sim$400 Mpc. It has been pointed out that weak BATSE GRBs appear to be correlated with galaxies out to distances of $\sim$155 Mpc with the limit determined by galaxy surveys [43].

A nearby population of long-lag, low-luminosity GRBs has previously been proposed based on the detections of GRB 980425, GRB 031203 and XRF 060218 [44, 45]. GRB 980425 has an isotropic-equivalent γ-ray energy release of $\sim 10^{48}$ ergs, approximately 3 orders of magnitude lower than that of "standard" GRBs, assuming its association with SN 1998bw [35] and redshift of $z = 0.0085$ [46]. XRF 060218, the second closest GRB localised to date, was detected at a redshift of $z = 0.033$ [47]. This burst had an extremely long duration ($T_{90} \sim 2100$ s) , a very low isotropic energy of $\sim 6 \times 10^{49}$ ergs and is classified as an XRF [48]. The distance to the long-lag GRBs can also be constrained by association and comparison with the two low luminosity bursts GRB 980425 ($\tau \sim 2.8$ s) and XRF 060218 ($\tau \sim 60$ s). The distances to GRB 980425 [35] and XRF 060218 [49]

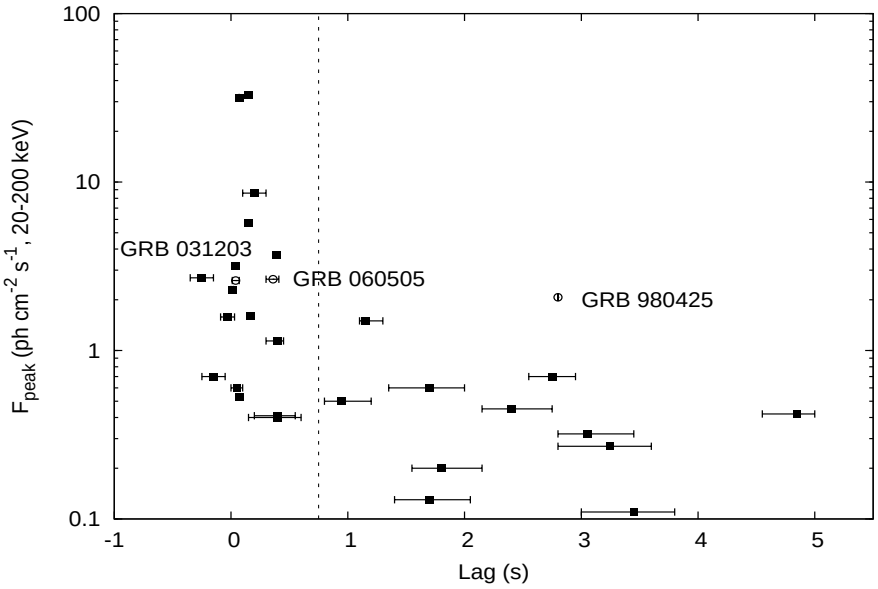

Figure 4: Spectral lag distribution of *INTEGRAL* GRBs as a function of peak flux (20–200 keV). The SN bursts GRB 980425 and GRB 031203 are identified and represented by open circles, as is GRB 060505 which does not have an associated SN. The dashed line indicates the separation between long and short-lag GRBs at $\tau_{2+3,1} = 0.75$ s.

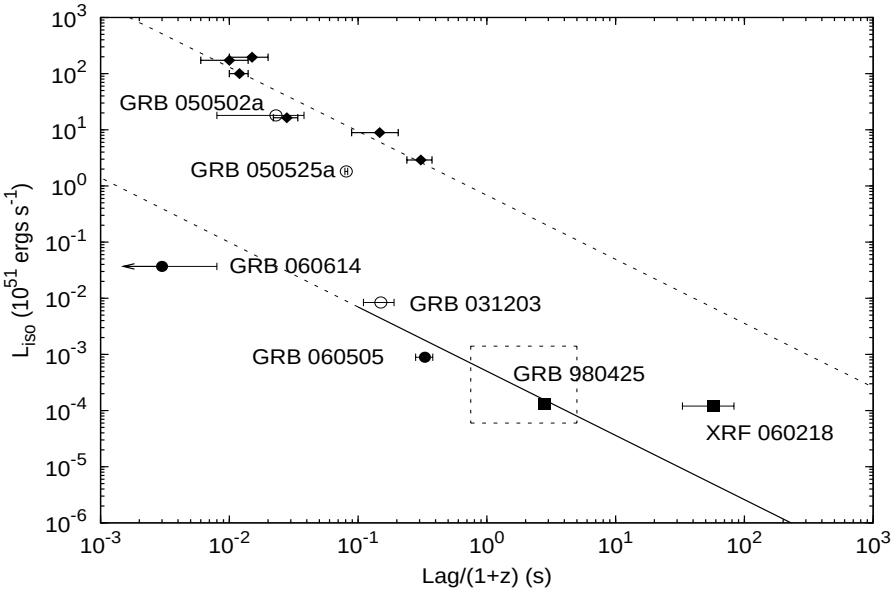

Figure 5: Isotropic peak luminosity ($\times 10^{51}$ ergs s^{-1}, 50–300 keV) as a function of spectral lag. The dashed line is the anti-correlation obtained for 6 bursts (diamonds) at known redshift [27]. The 3 *INTEGRAL* GRBs with a redshift and measured lag are represented by open circles, including the SN burst GRB 031203. The other low-luminosity SN bursts GRB 980425 and XRF 060218 are identified and represented by squares and the two GRBs without SNe by filled circles. The long-lag GRBs lie within the dashed box if they are at the adopted distance of 250 Mpc. The solid line is the proposed lag-luminosity relationship for the low-luminosity GRBs and extrapolates to short GRBs at low values of the lag, e.g. GRB 060614, which lies in the region of the plot occupied by short GRBs. No k-correction was applied to the data.

are 36 Mpc and 145 Mpc, respectively, and these bursts would have been detected in the FCFoV of IBIS to 135 Mpc and 290 Mpc. The association of the long-lag GRBs with the known low luminosity GRBs and with the supergalactic plane implies that they are at similar distances. The region marked with a box on the lag-luminosity plot (Fig. 4 (b)) contains the long-lag GRBs if they belong to the low luminosity population at an adopted distance of 250 Mpc. The box contains the prototype low luminosity GRB 980425 and is bracketed on one side by GRB 060218 and on the other by GRB 060505 ($\tau \sim 0.4$ s) and GRB 031203 ($\tau \sim 0.17$ s) and at short lag by GRB 060614 which lies in the region occupied by short GRBs [29]. With a long lag of ~ 2.8 s, GRB 980425 qualitatively

Table 2: Median properties of the 28 long-duration GRBs with a measured $\tau_{2+3,1}$, categorised into those with short lags ($\tau_{2+3,1} < 0.75$ s) and long lags ($\tau_{2+3,1} > 0.75$ s.)

	Short-lag GRBs	long-lag GRBs
Fraction of *INTEGRAL* GRBs	17/28	11/28
Median $\tau_{2+3,1}$ (s)	0.07	1.70
Median T_{90} (s)	27	50
Median F_{peak} (erg cm^{-2} s^{-1})	2.0×10^{-7}	4.0×10^{-8}
Median Fluence (erg cm^{-2})	2.0×10^{-6}	7.6×10^{-7}
% within $\pm 30^{\circ}$ SGB	41%	91%

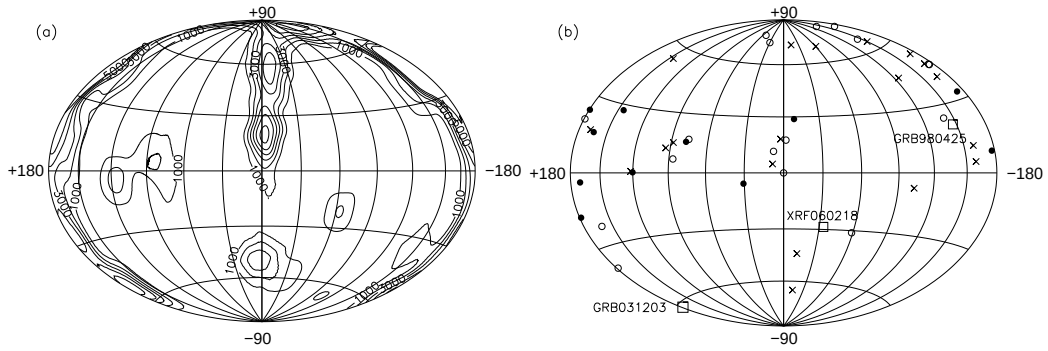

Figure 6: (a) *INTEGRAL* exposure map in supergalactic coordinates up to July 2007 (contours in units of kiloseconds). (b) The distribution of *INTEGRAL* GRBs in supergalactic coordinates; the open circles represent short-lag GRBs ($\tau_{2+3,1} < 0.75$ s) and filled-in circles those GRBs with long lags ($\tau_{2+3,1} > 0.75$ s). The 16 GRBs for which a lag could not be determined are denoted by an 'x', as are the XRFs which do not have a measured lag between 25–50 keV and 50–300 keV, and the short burst GRB 070707. Ten out of the 11 long-lag GRBs are within $\pm 30^\circ$ of the supergalactic plane.

follows the lag-luminosity trend but falls significantly below the relation in Fig. 4 (b) [38], as do GRB 031203 [10] and GRB 060218 [50]. The solid line in Fig. 4 (b) is the proposed lag-luminosity relationship for low-luminosity GRBs and is parallel to but shifted from the corresponding fit for the long cosmological GRBs by a factor of $\sim 10^3$.

GRBs have a long lag when a typical value of 0.1 s is redshifted by a large factor or alternatively is an intrinsic property of a low-luminosity GRB such as GRB 980425 and XRF 060218. The rate of $z > 5$ GRBs in IBIS has been modelled [51, 52] and is unlikely to be more than 1 or 2 GRBs in 5 years of observations. The long lag is therefore taken to be an intrinsic property of most of the long-lag GRBs indicating their low luminosity. The possibility that low luminosity GRBs could be part of the same population as cosmological GRBs or form a separate sub-energetic population with a much higher rate has been considered [49, 53]. The large number of long-lag GRBs detected with IBIS favours the latter conclusion and indicates that low redshift GRBs are dominated by the low luminosity class.

We evaluate the rate of such GRBs over the whole sky using the 8 long-lag *INTEGRAL* GRBs in the PCFoV at 50% coding (0.1 sr) over an exposure time of 4 years, adopting a distance of 250 Mpc and assuming that 2 of the 8 GRBs are not at low redshift. We obtain $2640\,\mathrm{Gpc}^{-3}\,\mathrm{yr}^{-1}$ which is $\sim$25% of the local rate of Type Ib/c SNe [49]. The major uncertainty in this estimate is the distance, where a change of only a factor of 2 increases or decreases this number by 8 to $21,100\,\mathrm{Gpc}^{-3}\,\mathrm{yr}^{-1}$ and $330\,\mathrm{Gpc}^{-3}\,\mathrm{yr}^{-1}$, respectively. The rate of low-luminosity GRBs at the adopted distance of 250 Mpc exceeds the upper limit of 3% or $< 300\,\mathrm{Gpc}^{-3}\,\mathrm{yr}^{-1}$ of Type Ib/c SN producing GRBs, which was derived assuming that all low luminosity GRBs would produce a SN and be as radio bright as the SN GRBs [49]. However, the low luminosity GRB 060605 has no associated SN to faint limits and is evidence for a quiet end for some massive stars [36, 54, 37]. A GRB may occur without a corresponding SN being observed if the ^{56}Ni does not have sufficient energy to escape the black hole or if the progenitor star has a low angular momentum.

The association of low luminosity GRBs with the supergalactic plane is not proof that they are associated with clusters of galaxies but indicates that clusters may play a role. It is interesting to

note that the rate of Type Ia SNe is higher in elliptical galaxies in clusters than in field ellipticals by a factor of $\sim$3 [55]. This effect is due to galaxy-galaxy interactions in clusters [56] either producing a small amount of young stars or affecting the evolution and properties of binary systems. In the latter case, there should also be an increase in the merger rate of white dwarfs or a white dwarf with a neutron star or black hole. A merger involving a white dwarf [57, 58] should produce a long GRB that is likely to be fainter than the formation of a black hole in cosmological GRBs. There will be no supernova in the merger of a white dwarf with a neutron star or black hole, and probably a faint afterglow. In addition, the merger could take place in the intercluster region without a host galaxy if the binary is ripped from its host in the merger interaction involving the cluster galaxies [59].

References

[1] P. Ubertini, F. Lebrun, G. Di Cocco, et al. IBIS: The Imager on-board INTEGRAL. *A&A*, 411:L131, November 2003.

[2] G. Vedrenne, J.-P. Roques, V. Schönfelder, et al. SPI: The spectrometer aboard INTEGRAL. *A&A*, 411:L63, November 2003.

[3] F. Lebrun, J. P. Leray, P. Lavocat, et al. ISGRI: The INTEGRAL Soft Gamma-Ray Imager. *A&A*, 411:L141, November 2003.

[4] C. Labanti, G. Di Cocco, G. Ferro, et al. The Ibis-Picsit detector onboard Integral. *A&A*, 411:L149, November 2003.

[5] J. M. Mas-Hesse, A. Giménez, J. L. Culhane, et al. OMC: An Optical Monitoring Camera for INTEGRAL. Instrument description and performance. *A&A*, 411:L261, November 2003.

[6] N. Lund, C. Budtz-Jørgensen, N. J. Westergaard, et al. JEM-X: The X-ray monitor aboard INTEGRAL. *A&A*, 411:L231, November 2003.

[7] S. Mereghetti, D. Götz, J. Borkowski, et al. The INTEGRAL Burst Alert System. *A&A*, 411:L291, November 2003.

[8] S. McGlynn, S. Foley, S. McBreen, et al. GRB 070707: the first short gamma-ray burst observed by INTEGRAL. *A&A*, 486:405, August 2008.

[9] S. Mereghetti, A. Paizis, D. Gotz, et al. *GCN 6927*, 2007.

[10] S. Y. Sazonov, A. A. Lutovinov, and R. A. Sunyaev. An apparently normal γ-ray burst with an unusually low luminosity. *Nature*, 430:646, August 2004.

[11] S. McBreen, L. Hanlon, S. McGlynn, et al. Observations of the intense and ultra-long burst GRB 041219a with the Germanium spectrometer on INTEGRAL. *A&A*, 455:433, August 2006.

[12] S. McGlynn, S. McBreen, L. Hanlon, et al. INTEGRAL and XMM-Newton observations of the low-luminosity and X-ray-rich burst GRB 040223. *Nuovo Cimento C*, 28:481, July 2005.

[13] P. Filliatre, S. Covino, P. D'Avanzo, et al. The weak INTEGRAL bursts GRB 040223 and GRB 040624: an emerging population of dark afterglows. *A&A*, 448:971, March 2006.

[14] S. Mereghetti, D. Götz, M. I. Andersen, et al. GRB 040403: A faint X-ray rich gamma-ray burst discovered by INTEGRAL. *A&A*, 433:113, April 2005.

[15] R. Marcinkowski, M. Denis, T. Bulik, et al. GRB 030406 - an extremely hard burst outside of the INTEGRAL field of view. *A&A*, 452:113, June 2006.

[16] C. Kouveliotou, C.A. Meegan, G.J. Fishman, et al. Identification of two classes of gamma-ray bursts. *ApJ*, 413:L101, August 1993.

[17] S. Foley, S. McGlynn, L. Hanlon, et al. Global characteristics of GRBs observed with INTEGRAL and the inferred large population of low-luminosity GRBs. *A&A*, 484:143, June 2008.

[18] C Guidorzi et al. *GCN 4504*, 2006.

[19] P. D'Avanzo et al. *GCN 2632*, 2004.

[20] J. X. Prochaska, J. S. Bloom, H.-W. Chen, et al. The Host Galaxy of GRB 031203: Implications of Its Low Metallicity, Low Redshift, and Starburst Nature. *ApJ*, 611:200, August 2004.

[21] L. J. Pellizza, P.-A. Duc, E. Le Floc'h, et al. GRB 050223: a dark GRB in a dusty starburst galaxy. *A&A*, 459:L5, November 2006.

[22] R. J. Foley, H.-W. Chen, J. S. Bloom, and J. X. Prochaska. *GCN 3483*, 2005.

[23] J. X. Prochaska, S. Ellison, R. J. Foley, and J. S. Bloom. *GCN 3332*, 2005.

[24] P. D'Avanzo, D. Malesani, S. Campana, et al. Discovery of the optical afterglow of XRF 040812: VLT and Chandra observations. *Nuovo Cimento C*, 121:1467, December 2006.

[25] A. de Luca, A. Melandri, P.A. Caraveo, et al. XMM-Newton and VLT observations of the afterglow of GRB 040827. *A&A*, 440:85, September 2005.

[26] J. Hakkila, T. W. Giblin, K. C. Young, et al. A Gamma-Ray Burst Database of BATSE Spectral Lag and Internal Luminosity Function Values. *ApJS*, 169:62, March 2007.

[27] J. P. Norris, G. F. Marani, and J. T. Bonnell. Connection between Energy-dependent Lags and Peak Luminosity in Gamma-Ray Bursts. *ApJ*, 534:248, May 2000.

[28] J. P. Norris and J. T. Bonnell. Short Gamma-Ray Bursts with Extended Emission. *ApJ*, 643:266, May 2006.

[29] N. Gehrels, J. P. Norris, S. D. Barthelmy, et al. A new γ-ray burst classification scheme from GRB060614. *Nature*, 444:1044, December 2006.

[30] D. L. Band. Gamma-Ray Burst Spectral Evolution through Cross-Correlations of Discriminator Light Curves. *ApJ*, 486:928, September 1997.

[31] J. M. Kommers, W. H. G. Lewin, C. Kouveliotou, et al. Supplement to the BATSE gamma-ray burst catalogs (Kommers+, 2001). *VizieR Online Data Catalog*, 213:40385, August 2001.

[32] B. E. Stern, Y. Tikhomirova, D. Kompaneets, et al. An Off-Line Scan of the BATSE Daily Records and a Large Uniform Sample of Gamma-Ray Bursts. *ApJ*, 563:80, December 2001.

[33] L. Chen, Y.-Q. Lou, M. Wu, J.-L. Qu, S.-M. Jia, and X.-J. Yang. Distribution of Spectral Lags in Gamma-Ray Bursts. *ApJ*, 619:983, February 2005.

[34] T. Yi, E. Liang, Y. Qin, and R. Lu. On the spectral lags of the short gamma-ray bursts. *MNRAS*, 367:1751, April 2006.

[35] T. J. Galama, P. M. Vreeswijk, J. van Paradijs, et al. An unusual supernova in the error box of the gamma-ray burst of 25 April 1998. *Nature*, 395:670, 1998.

[36] J. P. U. Fynbo, D. Watson, C. C. Thöne, et al. No supernovae associated with two long-duration γ-ray bursts. *Nature*, 444:1047, December 2006.

[37] S. McBreen, S. Foley, D. Watson, et al. The Spectral Lag of GRB 060505: A Likely Member of the Long-Duration Class. *ApJL*, 677:L85, April 2008.

[38] J. P. Norris. Implications of the Lag-Luminosity Relationship for Unified Gamma-Ray Burst Paradigms. *ApJ*, 579:386, November 2002.

[39] D. H. Hartmann, M. S. Briggs, and K. Mannheim. Searsch for Supergalactic Anisotropies in the 3B Catalog. In *American Institute of Physics Conference Series*, volume 384, page 397, 1996.

[40] O. Lahav, B. X. Santiago, A. M. Webster, M. A. Strauss, M. Davis, A. Dressler, and J. P. Huchra. The supergalactic plane revisited with the Optical Redshift Survey. *MNRAS*, 312:166, February 2000.

[41] C. Stoughton, R. H. Lupton, M. Bernardi, et al. Sloan Digital Sky Survey: Early Data Release. *AJ*, 123:485, January 2002.

[42] J. Abraham, P. Abreu, M. Aglietta, et al. Correlation of the highest energy cosmic rays with nearby extragalactic objects. *Science*, 318:938, November 2007.

[43] R. Chapman, N. R. Tanvir, R. S. Priddey, et al. How common are long gamma-ray bursts in the local Universe? *MNRAS*, 382:L21, November 2007.

[44] D. Guetta, R. Perna, L. Stella, and M. Vietri. Are All Gamma-Ray Bursts Like GRB 980425, GRB 030329, and GRB 031203? *APJL*, 615:L73, November 2004.

[45] F. Daigne and R. Mochkovitch. The low-luminosity tail of the GRB distribution: the case of GRB 980425. *A&A*, 465:1, April 2007.

[46] C. Tinney, R. Stathakis, R. Cannon, et al. *IAU Circular*, 6896, May 1998.

[47] N. Mirabal, J. P. Halpern, D. An, et al. GRB 060218/SN 2006aj: A Gamma-Ray Burst and Prompt Supernova at z = 0.0335. *ApJL*, 643:L99, June 2006.

[48] S. Campana, V. Mangano, A. J. Blustin, et al. The association of GRB 060218 with a supernova and the evolution of the shock wave. *Nature*, 442:1008, August 2006.

[49] A. M. Soderberg, S. R. Kulkarni, E. Nakar, et al. Relativistic ejecta from X-ray flash XRF 060218 and the rate of cosmic explosions. *Nature*, 442:1014, August 2006.

[50] E.-W. Liang, B.-B. Zhang, M. Stamatikos, et al. Temporal Profiles and Spectral Lags of XRF 060218. *ApJL*, 653:L81, December 2006.

[51] R. Salvaterra, S. Campana, G. Chincarini, et al. Gamma-ray bursts from the early Universe: predictions for present-day and future instruments. *MNRAS*, 385:189, March 2008.

[52] J. Gorosabel, N. Lund, S. Brandt, et al. The potential of INTEGRAL for the detection of high redshift GRBs. *A&A*, 427:87, November 2004.

[53] F. Virgili, E. Liang, and B. Zhang. Low-Luminosity Gamma-Ray Bursts as a Distinct GRB Population:A Monte Carlo Analysis. *astroph/0801.4751*, January 2008.

[54] S. Dado, A. Dar, A. De Rujula, and R. Plaga. Long gamma-ray bursts without visible supernovae: a case study of redshift estimators and alleged novel objects. *astro-ph/0611161*, November 2006.

[55] F. Mannucci, D. Maoz, K. Sharon, et al. The supernova rate in local galaxy clusters. *MNRAS*, 383:1121, January 2008.

[56] A. Boselli and G. Gavazzi. Environmental Effects on Late-Type Galaxies in Nearby Clusters. *PASP*, 118:517, April 2006.

[57] C. L. Fryer, S. E. Woosley, M. Herant, and M. B. Davies. Merging White Dwarf/Black Hole Binaries and Gamma-Ray Bursts. *ApJ*, 520:650, August 1999.

[58] A. King, E. Olsson, and M. B. Davies. A new type of long gamma-ray burst. *MNRAS*, 374:L34, January 2007.

[59] Y. Niino and T. Totani. Intracluster Short Gamma-Ray Bursts by Compact Binary Mergers. *ApJL*, 677:L23, April 2008.